SINTEF
PROCEEDINGS
2

Proceedings of the 12th International Conference on Computational Fluid Dynamics in the Oil & Gas, Metallurgical and Process Industries

# Progress in Applied CFD – CFD2017

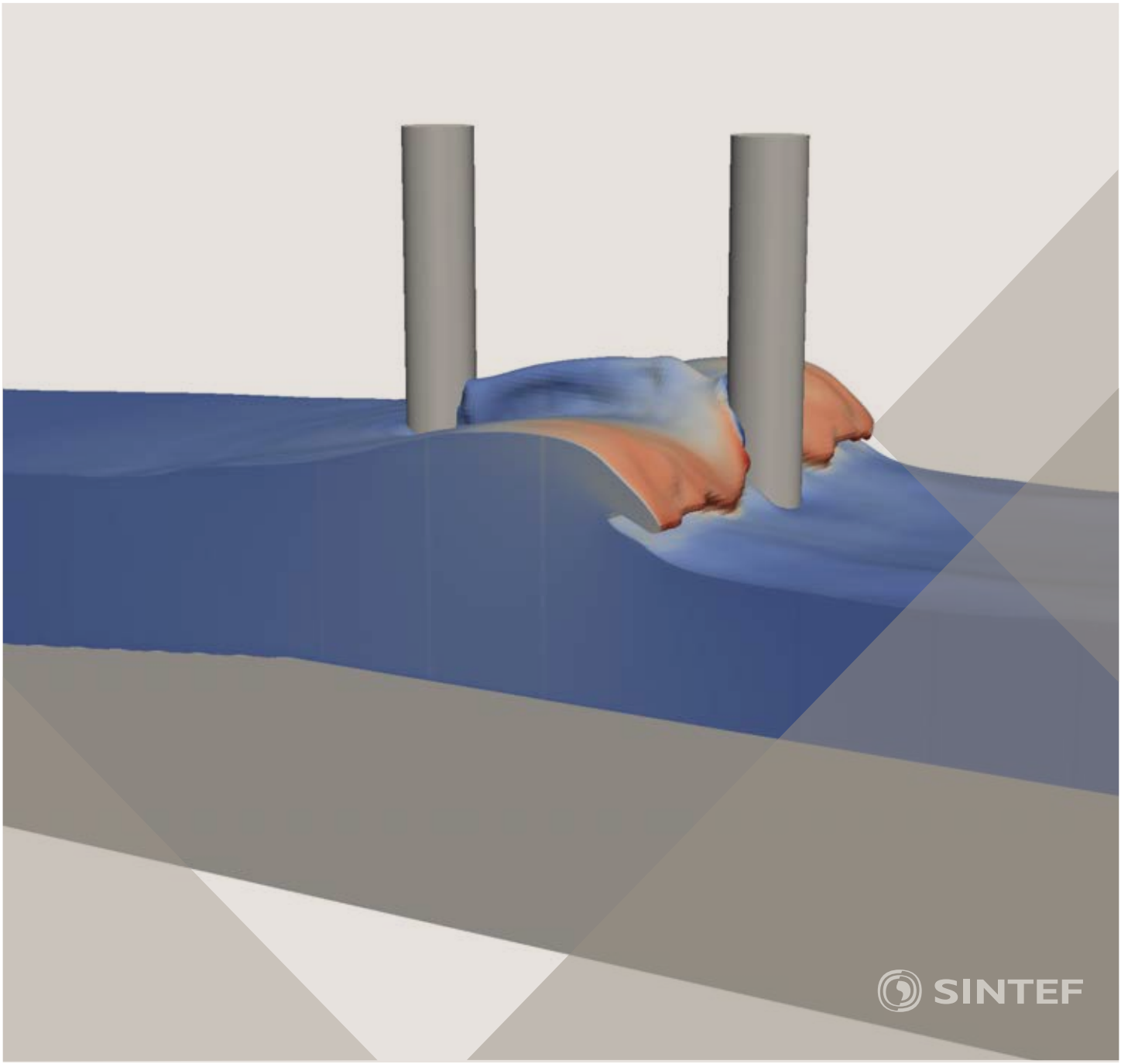

SINTEF Proceedings

Editors:
Jan Erik Olsen and Stein Tore Johansen

# Progress in Applied CFD – CFD2017

Proceedings of the 12th International Conference on Computational Fluid Dynamics in the Oil & Gas, Metallurgical and Process Industries

SINTEF Academic Press

SINTEF Proceedings no 2
Editors: Jan Erik Olsen and Stein Tore Johansen
**Progress in Applied CFD – CFD2017**
Selected papers from 10th International Conference on Computational Fluid Dynamics in the Oil & Gas, Metallurgical and Process Industries

Key words:
CFD, Flow, Modelling

Cover, illustration: Arun Kamath

ISSN 2387-4295 (online)
ISBN 978-82-536-1544-8 (pdf)



SINTEF Academic Press
Address: Forskningsveien 3 B
PO Box 124 Blindern
N-0314 OSLO
Tel: +47 73 59 30 00
Fax: +47 22 96 55 08

www.sintef.no/byggforsk
www.sintefbok.no

**SINTEF Proceedings**
SINTEF Proceedings is a serial publication for peer-reviewed conference proceedings on a variety of scientific topics.
The processes of peer-reviewing of papers published in SINTEF Proceedings are administered by the conference organizers and proceedings editors. Detailed procedures will vary according to custom and practice in each scientific community.

## PREFACE

This book contains all manuscripts approved by the reviewers and the organizing committee of the 12th International Conference on Computational Fluid Dynamics in the Oil & Gas, Metallurgical and Process Industries. The conference was hosted by SINTEF in Trondheim in May/June 2017 and is also known as CFD2017 for short. The conference series was initiated by CSIRO and Phil Schwarz in 1997. So far the conference has been alternating between CSIRO in Melbourne and SINTEF in Trondheim. The conferences focuses on the application of CFD in the oil and gas industries, metal production, mineral processing, power generation, chemicals and other process industries. In addition pragmatic modelling concepts and bio-mechanical applications have become an important part of the conference. The papers in this book demonstrate the current progress in applied CFD.

The conference papers undergo a review process involving two experts. Only papers accepted by the reviewers are included in the proceedings. 108 contributions were presented at the conference together with six keynote presentations. A majority of these contributions are presented by their manuscript in this collection (a few were granted to present without an accompanying manuscript).

The organizing committee would like to thank everyone who has helped with review of manuscripts, all those who helped to promote the conference and all authors who have submitted scientific contributions. We are also grateful for the support from the conference sponsors: ANSYS, SFI Metal Production and NanoSim.

Stein Tore Johansen & Jan Erik Olsen



Organizing committee:

Conference chairman: Prof. Stein Tore Johansen
Conference coordinator: Dr. Jan Erik Olsen
Dr. Bernhard Müller
Dr.Sigrid Karstad Dahl
Dr.Shahriar Amini
Dr.Ernst Meese
Dr.Josip Zoric
Dr.Jannike Solsvik
Dr.Peter Witt

Scientific committee:

Stein Tore Johansen, SINTEF/NTNU
Bernhard Müller, NTNU
Phil Schwarz, CSIRO
Akio Tomiyama, Kobe University
Hans Kuipers, Eindhoven University of Technology
Jinghai Li, Chinese Academy of Science
Markus Braun, Ansys
Simon Lo, CD-adapco
Patrick Segers, Universiteit Gent
Jiyuan Tu, RMIT
Jos Derksen, University of Aberdeen
Dmitry Eskin, Schlumberger-Doll Research
Pär Jönsson, KTH
Stefan Pirker, Johannes Kepler University
Josip Zoric, SINTEF

## CONTENTS

# MODELLING OF BUBBLE DYNAMICS IN SLAG DURING ITS HOT STAGE ENGINEERING

**Y. WANG[1]*, L. CAO[1,2], B. BLANPAIN[1], M. VANIERSCHOT[3], M. GUO[1]**

[1] KU LEUVEN Department of Materials Engineering, 3001 Leuven, BELGIUM

[2] UINVERSITY OF SCIENCE AND TECHNOLOGY BEIJING State Key Laboratory of Advanced Metallurgy, 100083 Beijing, CHINA

[3] KU LEUVEN Mechanical Engineering Technology TC, Campus Group T, 3001 Leuven, BELGIUM

* E-mail: yannan.wang@kuleuven.be

## ABSTRACT

Silica-rich additives are injected into the slag with $N_2/O_2$ as carrier gas to stabilize free lime in BOF (Basic Oxygen Furnace) steelmaking slag. In order to understand the mixing behaviour of the additives, bubble dynamics and momentum transfer are to be clarified at first. The objective of this work is to investigate the bubble breakup and the injected momentum transfer. To this purpose, a Volume of Fluid (VOF) two phase model was developed using ANSYS FLUENT software to study the dynamic breakup process of the gas phase and the velocity attenuation along the injected axis. Particle Image Velocimetry (PIV) measurements were used to validate the corresponding computational modelling. The validation between experimental measurements and computational modelling is reasonable in the turbulence model. Bubble breakup begins very quickly in the region near the inlet. The momentum contained in the gas phase is dissipated within a short distance from the inlet.

**Keywords:** bubble breakup; momentum transfer; computational modelling; particle image velocimetry

## NOMENCLATURE

*Greek Symbols*

$\alpha$ Volume fraction.

$\alpha_k$ $\alpha_\varepsilon$ Inverse effective Prandtl numbers.

$\varepsilon$ Turbulent dissipation rate, [$m^2/s^3$].

$\mu$ Dynamic viscosity, [kg/m.s].

$\mu_e$ Effective viscosity, [kg/m.s].

$\rho$ Mass density, [$kg/m^3$].

$\bar{\bar{\tau}}$ Stress tensor.

*Latin Symbols*

$A$ Inlet area, [$m^2$].

$C_\mu, C_{1\varepsilon}, C_{2\varepsilon}$ Constant, 0.0845, 1.42, 1.68, respectively.

$F$ Momentum source term, [$N/m^3$].

$\boldsymbol{g}$ Gravitational acceleration, [$m/s^2$].

$G_b$ Turbulence generation due to buoyancy.

$G_k$ Turbulence generation due to mean velocity gradient.

$k$ Turbulence kinetic energy, [$m^2/s^2$].

$p$ Pressure, [Pa].

$Q$ gas flow rate, [$Nm^3/min$].

$R_\varepsilon$ Additional term.

$S_\varepsilon$ Turbulence dissipation rate source term.

$S_k$ Turbulence kinetic energy source term.

$t$ Time, [s].

$T$ Temperature, [K].

$u_{in}$ Inlet velocity, [m/s].

$\mathbf{u}$ Velocity, [m/s].

$Y_M$ Contribution of the fluctuating dilatation.

*Sub/superscripts*

o Operating condition.

s Standard condition.

## INTRODUCTION

Currently, about 10 million tonnes of BOF (Basic Oxygen Furnace) slag is annually produced as a main by-product during steelmaking in Europe (Euroslag, 2017). Therefore, the use of BOF slag becomes a very urgent issue since it causes land occupation, environmental problems and resource waste. However, BOF slag valorization is restricted by its volume swelling during natural aging due to the presence of free lime (Liu *et.al*, 2016). In order to solve this problem, silica-rich additives, which are used to stabilize the free lime at high temperature, are injected into the liquid slag with nitrogen or oxygen gas as carrier gas through a top submerged lance. As a result, a buoyancy-driven flow in the slag pot is generated by gas injection, and the additives can move with the flow and react with free lime and other compounds.

In this whole process, the mixing efficiency is usually considered as one of the most important performance parameters, therefore, one of the main objectives is to attain a good mixing effect in the slag pot. To this end, it

is beneficial to clearly understand the way that the injected gas affects the mixing characteristics. Regarding this topic, bubble dynamics and momentum transport phenomena are closely involved. A large body of research has been directed at a similar topic in ladle metallurgy that is the interaction between gas bubble and liquid metal (*e.g.* Cloete *et.al*, 2009; Li *et.al*, 2008; Olsen and Cloete, 2009). Based on the references, it can be predicted that the stirring and mixing of slag in a treatment is also mainly attributed to buoyant potential energy in the form of gas bubbles with different sizes formed by gas jet breakup. In other words, the gas breakup in the slag pot is very important to the flow pattern and mixing characteristics.

The purpose of the present study is to build a computational model to study the gas jet breakup and the momentum transfer in the slag pot. This can lay the foundation for the further investigation of mixing characteristics in the slag pot. In order to validate the turbulence modelling, Particle Image Velocimetry (PIV) measurements in a scaled cubic vessel was performed, and a detailed comparison between experimental and numerical results is made.

## MODEL DESCRIPTION

For the sake of reducing the computational cost, only a transient two-dimensional and two-phase (*g-l*) model is developed in the present study. The Volume of Fluid (VOF) multiphase flow model is adopted to investigate the gas jet breakup due to the immiscible property and the sharp interface between gas bubble and liquid slag. The RNG *k-ε* turbulence model is applied to study the turbulence characteristics in the slag pot.

### Volume of Fluid Model

The VOF model is designed for two or more immiscible fluids which, in our case, are liquid slag and gas, respectively. In the VOF model, a single set of momentum equations is shared by the fluids, and the volume fraction of each of the fluids in each computational cell is tracked throughout the domain. The continuity and momentum equations are listed as follows:

Continuity equation

$$\frac{\partial \rho}{\partial t} + \nabla \cdot (\rho \mathbf{u}) = 0 \tag{1}$$

Momentum equation

$$\frac{\partial \rho \mathbf{u}}{\partial t} + \nabla \cdot (\rho \mathbf{u}\mathbf{u}) = -\nabla p + \nabla \cdot \left(\bar{\bar{\tau}}\right) + \rho \boldsymbol{g} + \boldsymbol{F} \tag{2}$$

In the VOF model, all variables and properties are shared by the phases and represent volume-averaged values. Therefore, the variables and properties in any given control volume are either purely representative of one of the phases, or representative of a mixture of the phases, which depends on the volume fraction values. In our two-phase system, the volume fractions of slag and gas sum up to unity. The volume-averaged density and viscosity can be represented by the following mathematical equations.

$$\alpha_{\text{slag}} + \alpha_{\text{gas}} = 1 \tag{3}$$

$$\rho = \alpha_{\text{slag}} \rho_{\text{slag}} + \alpha_{\text{gas}} \rho_{\text{gas}} \tag{4}$$

$$\mu = \alpha_{\text{slag}} \mu_{\text{slag}} + \alpha_{\text{gas}} \mu_{\text{gas}} \tag{5}$$

### RNG *k-ε* Model

RNG *k-ε* turbulence model is derived from the instantaneous Navier-Stokes equations, using a statistical technique called "renormalization group" (RNG) method. It has a similar form to the standard *k-ε* turbulence model, but includes several refinements. It is more appropriate for rapidly strained and swirling flows than the standard *k-ε* turbulence model, and it also provides an analytically derived differential formula for effective viscosity that accounts for low-Reynolds number effects (ANSYS, Inc., 2015).

The turbulence kinetics energy, $k$, and its dissipation rate, $\varepsilon$, in the RNG *k-ε* model are obtained from the following transport equations:

$$\frac{\partial}{\partial t}(\rho k) + \frac{\partial}{x_i}(\rho k u_i) = \frac{\partial}{\partial x_j}\left(\alpha_k \mu_e \frac{\partial k}{\partial x_j}\right) + G_k + G_b - \rho\varepsilon - Y_M + S_k \tag{6}$$

$$\frac{\partial}{\partial t}(\rho \varepsilon) + \frac{\partial}{\partial x_i}(\rho \varepsilon u_i) = \frac{\partial}{\partial x_j}\left(\alpha_\varepsilon \mu_e \frac{\partial \varepsilon}{\partial x_j}\right) + C_{1\varepsilon}\frac{\varepsilon}{k}(G_k + C_{3\varepsilon}G_b) - C_{2\varepsilon}\rho\frac{\varepsilon^2}{k} - R_\varepsilon + S_\varepsilon \tag{7}$$

The effective turbulent viscosity is solved by

$$\mu_e = \rho C_\mu \frac{k^2}{\varepsilon} + \mu \tag{8}$$

### Geometry and Operational Conditions

The geometry in the model consists of a slag pot and a lance. The slag pot is in the shape of a tapered cylinder and the lance is a simple cylinder. Liquid slag is contained in the slag pot with a certain height. The lance is submerged into the liquid slag from the slag level to a specific depth in the centre position. The dimensions and physical properties and operational conditions are listed in Table 1, 2 and 3, respectively. Since it is a symmetrical geometry, only half of it was built. The total node number is around 36000, which is large enough to obtain a sharp interface between gas bubble and liquid slag. The geometry with the grid is depicted in Figure 1.

**Table 1**: Geometrical dimensions of the pot.

| | |
|---|---|
| Top diameter, mm | 3360 |
| Bottom diameter, mm | 2390 |
| Height, mm | 3558 |
| Lance diameter, mm | 40 |

**Table 2**: Physical properties.

| | |
|---|---|
| Density of slag, kg/m$^3$ | 3000 |
| Density of air, kg/m$^3$ | 0.567* |
| Viscosity of slag, kg·m$^{-1}$·s$^{-1}$ | 0.100 |
| Viscosity of air, kg·m$^{-1}$·s$^{-1}$ | 8.9e-5 |
| Surface tension of slag/gas, N/m | 0.55 |

"*" indicates a lower air density due to the high temperature in real case.

**Table 3**: Operating conditions.

| | |
|---|---|
| Air flow rate, $Nm^3/min$ | 3 |
| Inlet velocity, m/s | 50.0 to 84.5 |
| Operating temperature, K | 1873 |
| Operating pressure, Pa | 3e5 to 5e5 |
| Lance depth, mm | 1000 |
| Height of slag level, mm | 3000 |

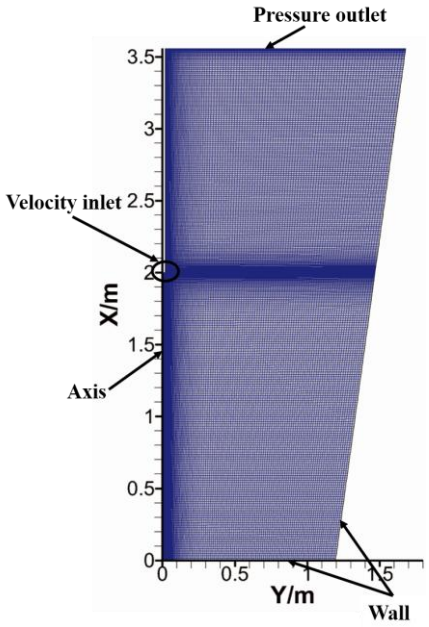


**Figure 1:** Geometry with grid.

The heat transfer is not in the scope of this study, therefore, the temperature gradient is neglected, which means that a uniform temperature field is assumed in this simulation. The inlet velocity of air is calculated based on the following equation.

$$u_{in} = \frac{Q_o}{A} = \left(\frac{p_s T_o}{p_o T_s}\right)\frac{Q_s}{A} \qquad (9)$$

## Numerical Method

This model is implemented in FLUENT 16.2. Velocity inlet and pressure outlet boundary conditions are adopted for this simulation. For the solution methods, the Pressure-Implicit with Splitting Operators (PISO) pressure-velocity coupling scheme is used, which is recommended for a transient problem. PISO scheme has its own advantages that allows higher under-relaxation values for both momentum and pressure, leading to less iterations and faster convergence. In the spatial discretization part, the PREssure Staggering Option (PRESTO!) scheme and second order upwind scheme are performed for pressure and momentum, respectively. Convergence is monitored by means of the unscaled residual of the continuity equation. The reason is that the continuity equation is the most difficult one to converge. In this study, it is considered that the residual of the continuity equation must drop at least 3 orders of magnitude to obtain a sufficient accuracy. Therefore, the convergence criterion less than $10^{-7}$ is chosen when the time step size is $1\times10^{-4}$.

The simulations were uploaded to a High Performance Computing (HPC) cluster. 2-5 nodes with 40-100 processors were required for the simulations.

## TURBULENCE MODEL VALIDATION

In order to validate the RNG $k$-$\varepsilon$ turbulence model, PIV measurements and the corresponding simulations were conducted beforehand.

### Experimental setup

In the measurements, paraffin oil and compressed air are used to form a two-phase system. The vessel made of transparent glass is cubic shape with dimensions of 135 × 135 × 195 mm. A glass pipe with inner diameter of 5 mm taken as the top lance is also placed in the centre of the vessel. The operating conditions and physical properties are listed in Table 4.

The flow field in the vessel is measured by Time-Resolved PIV (TR-PIV). Since the vessel is axisymmetric, only the left zone is of interest. It can also be easily predicted that the liquid mainly flows in the upper part based on two considerations, one of which is that the upper part liquid is driven by the rising air, and the other one is that the injected air cannot penetrate very deeply, so the liquid in the lower part is almost still. Therefore, the selected area to be measured is located in the upper left part of the median plane, which is shown in Figure 2. A PIV laser (wavelength 527 nm, pulse energy 10 mJ @ 1000 Hz) from NewWave is employed to generate a laser sheet with a thickness of 0.5 mm which exactly overlaps the median plane of the vessel. The flow is seeded with hollow PMMA particles of diameters between 20 and 50 μm. The particles are coated by Rhodamine B to exhibit fluorescence, which can help increase the signal to noise ratio when the back light of the laser sheet is filtered out by an optical filter. In order to correct for light refraction, the PIV system was calibrated by means of placing a calibration plate in the measured flow field, and the plate exactly overlaps the laser sheet. The images are recorded by a CMOS camera (HighSpeedStar 5) with a resolution of 1024 × 1024 pixels. The calculation of velocity vector is processed by the Davis 8.1 software (LaVision GmbH). Further data processing is executed by Matlab software (R2016a) using specific code.

The corresponding numerical simulation is established with the same multiphase flow model (VOF) and the turbulence model (RNG $k$-$\varepsilon$). The half meshing with around 5800 nodes is shown in Figure 4. The solution methods are also kept the same. These can ensure consistent approaches to the following simulation of flow field in the slag pot.

**Table 4**: Operating parameters and physical properties.

| | |
|---|---|
| Air flow rate, NL/h | 300 |
| Inlet velocity, m/s | 4.25 |
| Submerged depth, m | 0.044 |
| Height of oil level, m | 0.164 |
| Density of oil, $kg/m^3$ | 880 |
| Density of air, $kg/m^3$ | 1.225 |
| Viscosity of oil, $kg\cdot m^{-1}\cdot s^{-1}$ | 0.065 |
| Viscosity of air, $kg\cdot m^{-1}\cdot s^{-1}$ | 1.789e-5 |
| Surface tension of oil/air, N/m | 0.026 |

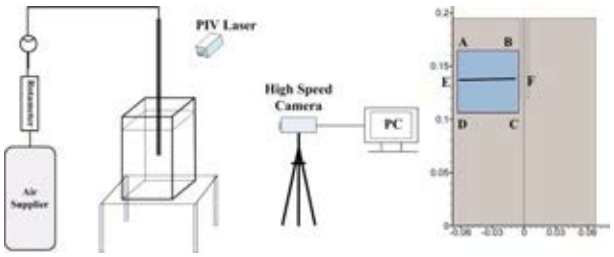


**Figure 2**: Schematic of the experimental setup and the measured area: A (-0.063, 0.164); B (-0.005, 0.164); C (-0.005, 0.106); D (-0.063, 0.106); E (-0.063, 0.135); F (-0.005, 0.135).

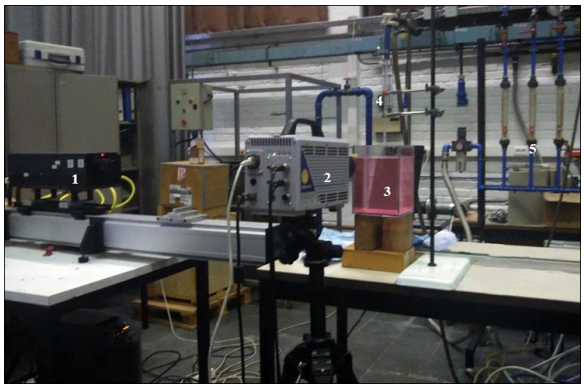


**Figure 3**: Photograph of the experimental setup.
(1: laser generator; 2: highspeed camera; 3: paraffin oil with PMMA particles; 4: glass pipe; 5: rotameter)

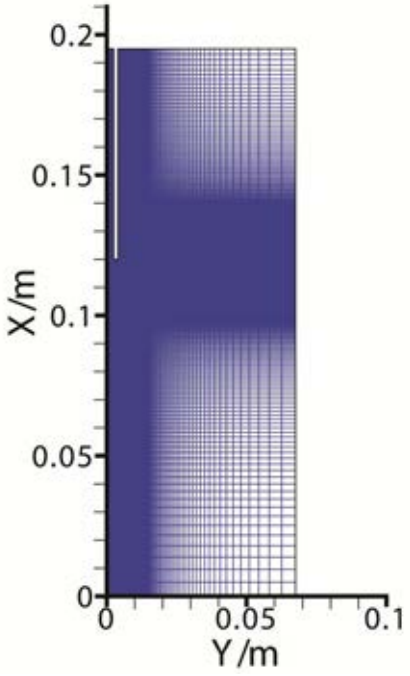


**Figure 4**: Meshing of the computing domain.

## RESULTS

### Model Validation

The turbulence model in numerical simulation is verified with experimental data by comparing the time-averaged velocity fields in the domain. The representative case with air flow rate of 300 NL/h is employed here, and the results are presented in Figure 5 and 6, respectively.

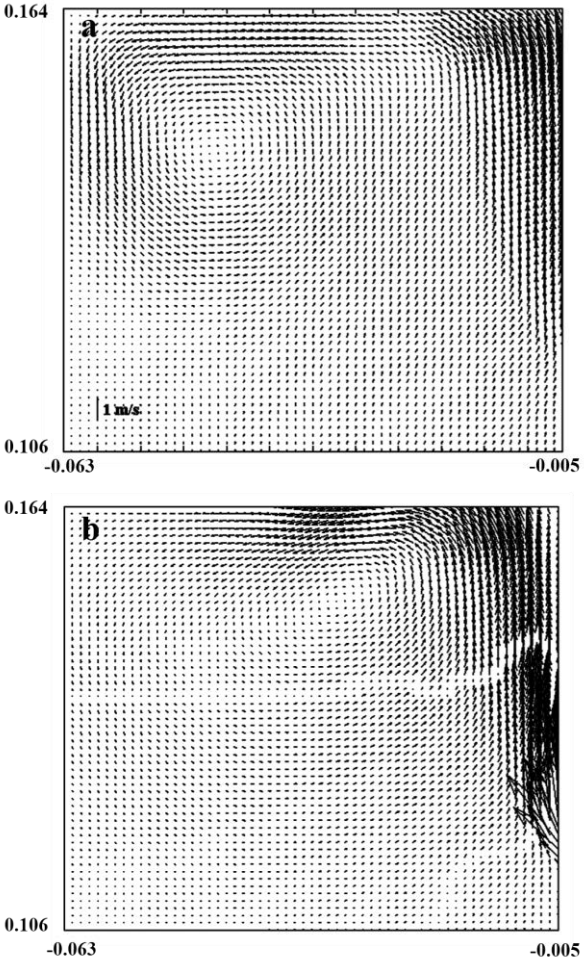


**Figure 5:** Comparison of the experimentally and numerically obtained time-averaged velocity fields (air flow rate: 300 NL/h). (a) velocity field of the PIV measurements and (b) velocity field of the numerical simulations.

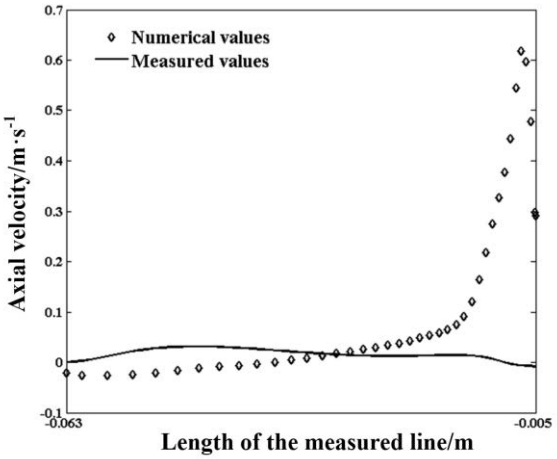


**Figure 6**: Axial velocity profile of the measured line EF shown in figure 2.

It can be seen from Figure 5 that a circulation zone consisting of a counter-clockwise rotating vortex is formed in the middle of the measured zone in the measurement, and a similar one can be observed in the corresponding numerical simulation, despite of a deviation of the location of the vortex centre. There may be a reason to explain it. Because a 2D axisymmetric model is used in this study, the domain will sweep 360 degree along *x*-axis by default, which makes the

computing domain more like a cylinder. However, the model in this study in a cubic one. This may be the reason for the deviation of the vortex centre. A further work of the corresponding 3D modelling will be established to determine the reason. It also can be observed that a large discrepancy appears in the very right region. This is because this measured region is very close to the gas pipe, and the gas bubbles rising along with this pipe posed serious influence on the measurement due to the refractive issues. In other words, the obtained data in the region close to the gas pipe is hardly reliable.

The axial velocity profile of the measured line shown in Figure 2 is depicted in Figure 6. Clearly, this is a big deviation in the right part, and the reason of it has been explained in the last paragraph. Apart from this, the rest seems acceptable since only minor errors appear. This may be attributed to the coarse meshing.

In conclusion, the results are still convincing since a similar circulation in the middle of the measured region and an acceptable quantitative validation can be observed, which means the flow patterns in the experiment and modelling resemble each other. However, there is, for sure, some space to improve the model. Based on the above description, the influence of the gas injection on the flow field is reasonably validated.

## Bubble Formation

In the slag valorization process, gas stirring is a key step. When the gas is injected into the slag through a submerged top lance, the continuous gas phase splits into discrete gas bubbles that move upward with high velocity. Soon a conical plume consisting of gas bubbles and liquid is shaped in the upward path. It is the moving bubbles that transfer momentum to the surrounding liquid and make the system stirred. Hence, gas breakage into bubbles is very important for transport phenomena in multiphase flow. For our study, gas breakage is the precondition for a better mixing, and it is well worth being investigated.

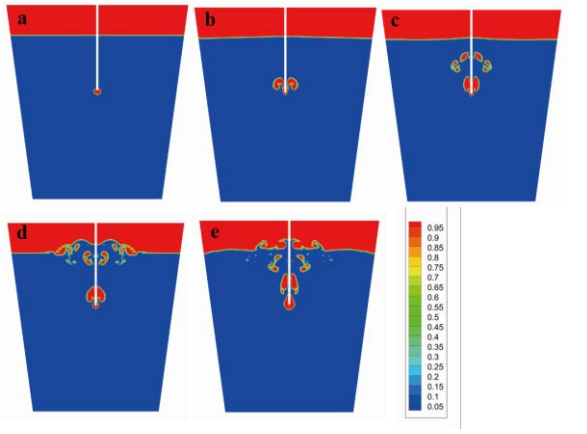


**Figure 7:** Gas bubble formation represented by the gas volume fraction (a: 0.02 s; b: 0.3 s; c: 0.75 s; d: 1.58 s; e: 2.70 s).

Figure 7 shows the dynamic breakage process of the gas phase in the slag pot. As can be seen in Figure 7(a), the gas phase comes out of the inlet and forms an approximate circle. The upper part of the circle is a little deformed due to the pressure difference along the bubble surface. Later a dumbbell shape with a narrow neck forms near the inlet as the pressure difference continues increasing. Finally the gas phase splits into several gas bubbles. The gas bubbles keep moving up and can break up into even smaller bubbles.

It can be concluded that the gas phase begins breakup very soon near the inlet region, where large velocity gradient and turbulence kinetics energy exist. This will be further described in the following section. The formed bubbles can have secondary or several times breakup caused by turbulent eddies during rising up. Many studies in regard to bubble breakup can be found in chemical engineering, most of which, however, were performed in low temperature systems (*e.g.* Xing *et.al*, 2015; Luo and Svendsen, 1996; Hengel *et.al*, 2005). Nonetheless, these existing studies can supply important references for further investigation.

## Momentum Characteristics

In ladle metallurgy, the gas phase is injected from the bottom through plugs, and the gas flow rate is smaller compared to that in slag valorization. It has been proved that the injected momentum in ladle metallurgy is dissipated within a very short distance (Krishnapisharody and Irons, 2013). In Ausmelt TSL application, the gas phase is injected from the top via a top submerged lance. (Hoang *et.al*, 2009; Wood *et.al*, 2011). A violent stir can be obtained in the bath. Therefore, it is necessary to make clear if the injected momentum in the slag valorization can make an important contribution to system stirring. Three cases with initial inlet velocity of 84.5, 62.5 and 50.0 m/s, respectively, are discussed here. The time-averaged velocity and instantaneous results of turbulent kinetic energy and dissipation rate along the axis at 10.0 s are presented in Figure 8, 9 and 10, respectively.

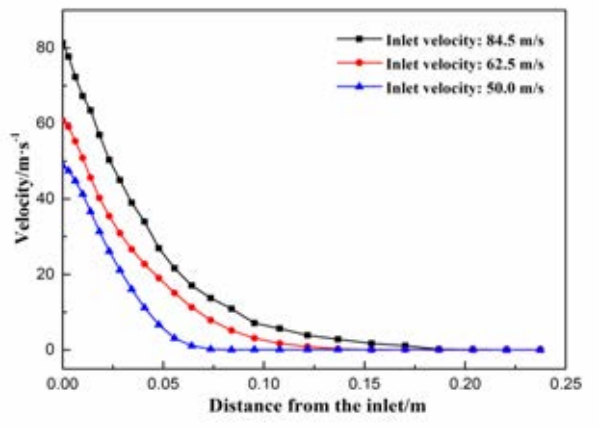


**Figure 8:** Velocity attenuation along the injected axis

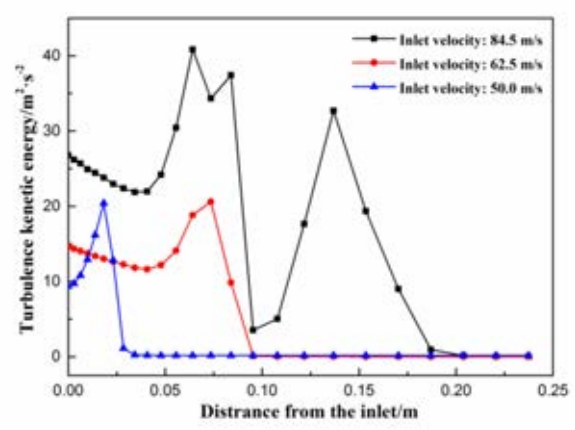


**Figure 9**: Attenuation of turbulence kinetic energy along the injected axis

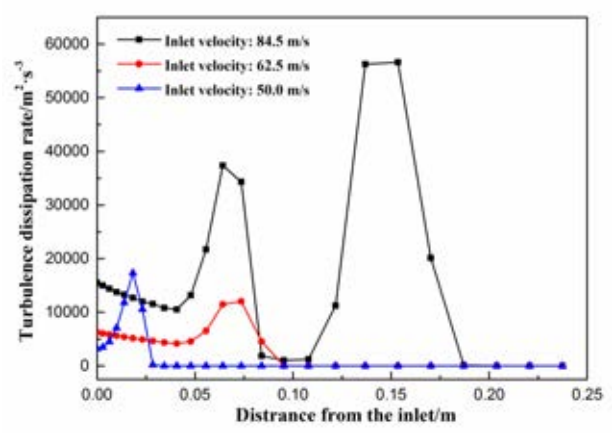


**Figure 10**: Attenuation of turbulence dissipation rate along the injected axis

The penetration depth is increased with increasing inlet velocity, which is clearly shown in Figure 8. However, the penetration depth is still quite small compared to the distance between the inlet and the bottom wall which is 2 m. This is because the density difference between the gas phase and slag is huge. Even with a very large inlet velocity, *e.g.* 84.5 m/s, the penetration depth is small compared to the slag bath height.

In Figure 9 and 10, the turbulence kinetic energy and it dissipation rate are depicted along the injected axis. The attenuations are consistent with the velocity attenuation, so the turbulence kinetic energy is dissipated in a short distance, which corresponds to other researchers' work mentioned previously. It can also be concluded that the turbulence kinetics energy and its dissipation rate are very unstable in this short distance according to the sharp peaks. Therefore, it can be imaged that turbulence in the adjacent area of the inlet is very violent. This can explain why the gas phase can split easily into bubbles in this region.

Now that it has been proved the injected momentum is limited in stirring the slag, it can be inferred that the flow is mainly driven by buoyancy of gas bubbles. This can be easily understood since the pressure difference between the top and bottom surfaces of bubbles is so large, which makes the bubble move upward with high velocity, and this high velocity can be transferred to the surrounding slag through interphase interactions. This is how gas bubbles drive liquid slag flow in the slag pot.

## CONCLUSIONS

The turbulence model used in our numerical simulation is quantitatively validated by comparing the velocity fields obtained from experiment and simulation, and the result is reasonable.

VOF model can successfully capture the dynamic breakup process of the gas phase. In our study, the gas phase breaks up into gas bubbles very quickly in the region adjacent to the inlet and the formed bubbles can undergo secondary or several times breakage while rising up.

The injected momentum is found to be dissipated in a short distance, very close to the inlet as indicated with measurements of the velocity attenuation and turbulence kinetic energy attenuation. This is consistent with the findings in the ladle metallurgy.

## ACKNOWLEDGEMENT

The financial support from IWT Grant 140514 (Belgium) and computer support from HPC (KU Leuven) are highly acknowledged. Yannan Wang and Lingling Cao want to thank the support of the China Scholarship Council (CSC).

## REFERENCES

ANSYS, Inc., (2015), "Ansys fluent theory guide".

CLOETE, S.W.P., EKSTEEN, J.J. and BRADSHAW, S.M., (2009), "A mathematical modelling study of fluid flow and mixing in full-scale gas-stirred ladles", Progress in Computational Fluid Dynamics, 9, 345-356.

Euroslag: www.euroslag.com. Accessed on 20 February, 2017.

HOANG, J., REUTER, M. A., MATUSEWICZ, R., HUGHES, S. and PIRET, N., (2009), "Top submerged lance direct zinc smelting", Minerals Engineering, 22, 742-751.

HENGEL, E.I.V., DEEN, N.G. and KUIPERS, J.A.M., (2005), "Application of coalescence and breakup models in a discrete bubble model for bubble columns", Industrial Engineering Chemistry Research, 44, 5233-5245.

KRISHNAPISHARODY, K and IRONS, G.A., (2013), "A critical review of the modified Froude number in ladle metallurgy", Metallurgical and Materials Transaction B, 44B, 1486-1498.

LI, B., YIN, H., ZHOU, C. and TSUKIHASHI, F., (2008), "Modelling of three-phase flows and behaviour of slag/steel interface in an argon gas stirred ladle", ISIJ International, 48, 1704-1711.

LIU C., GUO, M., PANDELAERS, L., BLANPAIN, B. and HUANG, S., (2016), "Stabilization of free lime in BOF slag by melting and solidification in air", Metallurgical and Materials Transactions B, 47B, 3237-3240.

LUO, H. and SVENDSEN, F., (1996), "Theoretical model for drop and bubble breakup in turbulent dispersions", AIChE Journal, 42, 1225-1233.

OLSEN, J.E. and CLOETE, S., (2009), "Coupled DPM and VOF model for analyses of gas stirred ladles at higher gas rates", 7th International Conference on CFD in the Minerals and Process Industries, CSIRO, Melbourne, Australia, December 9-11.

WOOD, J., CREEDY, S., MATUSEWICZ, R. and REUTER, M, (2011), “Secondary copper processing using Outotec Ausmelt TSL technology”, Proceedings of MetPlant, 460-467.

XING, C., WANG, T. and WANG, J., (2015), “A unified theoretical model for breakup of bubbles and droplets in turbulent flows”, AIChE Journal, 61, 1391-1403.